ACS APPLIED MATERIALS & INTERFACES

Research Article

Cite This: ACS Appl. Mater. Interfaces 2019, 11, 1321−1334

www.acsami.org

Multifunctional Polystyrene Core/Silica Shell Microparticles with Antifouling Properties for Bead-Based Multiplexed and Quantitative Analysis

Dominik Sarma,[†,‡] Peter Carl,[†,‡] Estela Climent,[†] Rudolf J. Schneider,[†,§] and Knut Rurack*[,†]

[†]Department of Analytical Chemistry; Reference Materials, Bundesanstalt für Materialforschung und -prüfung (BAM), Richard-Willstätter-Straße 11, 12489 Berlin, Germany

[‡]Department of Chemistry, Humboldt-Universität zu Berlin, Brook-Taylor-Straße 2, 12489 Berlin, Germany

[§]Technische Universität Berlin, Straße des 17. Juni 135, 10623 Berlin, Germany

Supporting Information

ABSTRACT: Commercial bead-based assays are commonly built upon polystyrene particles. The polymeric carrier can be encoded with organic dyes and has ideal material properties for cytometric applications such as low density and high refractive index. However, functional groups are conventionally integrated during polymerization and subsequent modification is limited to the reactivity of those groups. Additionally, polystyrene as the core material leads to many hydrophobic areas still being present on the beads' surfaces even after functionalization, rendering the particles prone to nonspecific adsorption during an application. The latter calls for several washing steps and the use of additives in (bio)analytical assays. In this contribution, we show how these limitations can be overcome by using monodisperse polystyrene (PS) core/silica (SiO_2) shell particles (SiO_2@PS). Two different hydrophobic BODIPY (boron−dipyrromethene) dyes were encapsulated inside a poly(vinylpyrrolidone) (PVP) -stabilized polystyrene core in different concentrations to create 5-plex arrays in two separate detection channels of a cytometer. A subsequent modification of the silica shell with an equimolar APTES/PEGS (aminopropyltriethoxysilane/polyethylene glycol silane) blend added multifunctional properties to the hybrid core/shell microparticles in a single step: APTES provides amino groups for the attachment of a caffeine derivative (as a hapten) to create antigen-coupled microspheres; the PEG moiety effectively suppresses nonspecific binding of antibodies, endowing the surface with antifouling properties. The particles were applied in a competitive fluorescence immunoassay in suspension, and a highly selective wash-free assay for the detection of caffeine in beverages was developed as a proof of concept.

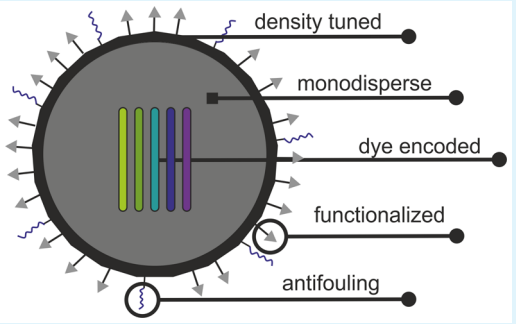

KEYWORDS: *core−shell particles, bead-based assay, multiplex, antifouling surface, mixed surface*

INTRODUCTION

The use of encoded spherical microparticles (beads) as the solid carrier in (bio)analytical cytometric assays is well-suited for the quantitative detection of multiple analytes under high-throughput conditions, because such assays rely on fast reaction kinetics and the handling of samples with low volume.[1−4] These features contributed to their ever-increasing popularity in biomedical diagnostics and drug development, applications in which short assay processing times are essential and only limited amounts of sample material are available.[5,6] More recently, the immunochemical detection of small-molecule analytes for which the corresponding mono- or polyclonal antibodies are available became increasingly popular in food and environmental analysis with special focus on wastewater and agricultural samples.[7−9] Today, commercial bead-based platforms such as the Luminex xMAP or the BD Cytometric Bead Array represent the most commonly employed systems for suspension array technology (SAT). Here, the beads are provided in the form of functionalized and dye-encoded polystyrene (PS) particles with diameters of 5.5 and 7 μm.[10,11] The successful establishment of SAT led to other suppliers also offering encoded beads in various sizes for open platform integration in cytometric or fluorescence imaging formats, e.g., the Plex Red4 kit from PolyAn GmbH, Berlin, Germany, or Quantumplex from Bangs Laboratories, Inc., Fishers, IN. However, three major drawbacks using polystyrene carriers in multiplexed bead arrays can be identified.

(i) Beads of comparatively large sizes with diameters >3 μm are required to guarantee acceptable processing times when using centrifugation during washing or functionalization steps.[12]

Received: June 20, 2018
Accepted: December 3, 2018
Published: December 3, 2018

(ii) The encoding with organic dyes is limited to low- (number of parameters <5) or medium-plex panels (number of parameters <500), because dyes tend to aggregate at higher concentrations, and/or if different dyes are used, their spectral overlap in typical detection windows precludes higher-order multiplexing.[13]

(iii) The beads often show a strong tendency for nonspecific binding of biomacromolecules, potentially leading to low signal-to-noise ratios (S/N) or the generation of false-positive signals.[14]

Most of the published work on novel particle designs for cytometric applications focused on drawback (ii), i.e., they aim at an extension of the multiplexing capacity. For example, Gu, Xu et al. prepared a 100-code library based on a complex host−guest assembly approach to overcome spectral interferences from multiple dyes incorporated in the same domain.[15,16] Lu et al. reported lifetime encoding and on-the-fly decoding in scanning cytometry.[17] Whether such an approach has a "significant multiplexing capacity", despite the considerable computation time that the decoding of higher-plex lifetime encoded arrays would require, remains to be shown. An alternative to organic fluorophores for encoding are quantum dots (QDs). These semiconductor nanocrystals possess advantageous fluorescence properties such as high quantum yields and narrow emission bands while being excitable in a broad spectral window.[18] Despite these promising features, the use of QDs is still waiting for a breakthrough. Recent research that promoted QD encoding stayed with triplexing, revealing no substantial benefit.[19] Besides fluorescence, other approaches such as Raman spectral encoding or graphically encoded microcarriers have been proposed to propel SAT beyond the current limit of 500 codes.[20] However, whereas Raman encoding is still in its infancy, lithographic codes cannot be decoded with conventional flow cytometry.[21−23]

It is obvious that many attempts so far showed only moderate success to surpass the 500-codes limit in SAT. They will thus hardly replace well-plate formats or microarray technologies as the classical "workhorses" in qualitative high-throughput screening (HTS) applications such as early drug discovery or genome-related screening (microRNA profiling, DNA sequencing). With respect to quantitative analysis, on the other hand, multiplexed systems are limited to the detection of a few analytes in parallel in either well-plate formats or microarray technologies, mainly because of cross- and shared reactivity issues.[24,25] Consequently, the strengths of many of the low- to medium-plex bead arrays proposed so far can perhaps be much better exploited in quantitative assays. This was the main reason for us to address aspects related to drawback (iii) in this work: nonspecific binding.

Nonspecific binding can be reduced by using additives such as poly(vinyl alcohol) or commercial blocking formulations when simple polystyrene beads are employed. However, further washing steps are required during assay processing.[14,26] A more convenient route to suppress nonspecific binding on beads is to endow their surface with antifouling properties. This can be achieved through the attachment of hydrophilic polyethylene glycol (PEG) or zwitterionic moieties such as sulfobetaines.[27] However, because commercial beads usually express a single functional group on their surface, mostly an amino or a carboxylic acid group, multistep procedures, heterobifunctional linkers, or partial functionalization routes are commonly needed for introducing a second (antifouling) function to the microparticles' surface.[28−30] In-situ formation of PEGylated polymer beads using, for instance, PEG comonomers during polymerization has been reported in methodological articles. Their application features however were not studied.[31] A straightforward, single-step and modular synthesis protocol to equip encoded beads with a bi- or multifunctional surface, offering functional groups for coupling and against fouling, is thus highly desirable. Ideally, such beads would have sizes around 1 μm to increase reaction kinetics and allow for small reaction volumes.

As we will show in this contribution, access to all these features is possible when polystyrene (PS) core/silica (SiO_2) shell (SiO_2@PS) particles are used. Such hybrids allow to combine the material features of PS as a core and provide a defined silica shell for controlled postmodification using silane chemistry. APTES provides amino groups for the attachment of a caffeine hapten derivative to create antigen-coupled microspheres; polyethylene glycol silane (PEGS) introduces poly(ethylene glycol) moieties, endowing the surface with antifouling properties to suppress nonspecific binding. Surprisingly, published work on SiO_2@PS beads did not yet make full use of the chemical flexibility offered by a silica surface. Concerning the dedicated surface functionalization of encoded beads, for instance, Wu et al. prepared silica-coated melamine-formaldehyde resins for bead-based assays. They focused on the preparation of colored beads and functionalized the surface only with 3-aminopropyltriethoxysilane (APTES) as the single silane.[32−34] Jun et al. used PS beads decorated with silver nanoparticles (NPs) that were encapsulated into a silica shell containing Raman reporter molecules for SERS (surface enhanced Raman scattering) encoding. However, again, APTES was used as the sole silane for surface functionalization.[35] Also in the case of PS cores doped with QDs for SAT, Cao and co-workers only implemented a single functional group after encapsulation of the microparticle cores with a silica shell.[36] Based on the layer-by-layer approach to core/shell particles,[37] Wilson et al. encoded PS beads with layers of QDs before assembling a final layer of SiO_2 NPs. This layer, however, was also only modified with APTES.[38] To elucidate the possibilities lying dormant with silica surface modification, we combined here our expertise in SiO_2@PS particle design,[39,40] mixed silane surfaces,[41,42] and dye-doped polymer particles[43] to develop APTES- and PEGS-expressing encoded beads that constitute the basis of a straightforward 5-plex array. We employed the beads in an exemplary mix-&-read competitive immunoassay for the psychoactive compound caffeine (CAF). The determination of CAF in beverages such as energy drinks is under legislation of the European Union.[44] Quantitative, fast and simple methods for the monitoring of CAF contents in such foodstuffs are thus required. We realized quantitative determination of CAF in beverages using a wash-free protocol with flow cytometry read-out with negligible nonspecific binding due to the antifouling properties of the beads' silica surface.

EXPERIMENTAL SECTION

Polystyrene Core Synthesis. Two batches of poly(vinylpyrrolidone) (PVP)-stabilized polystyrene core particles were prepared, a small-scale batch in ethanol as described in Sarma et al.[40] and a larger-scale batch with 10-fold increased reaction volume as described before.[39] Besides PVP40 (PVP with an average molecular weight of ~40 kDa) used for both batches, isopropanol instead of

DOI: 10.1021/acsami.8b10306
ACS Appl. Mater. Interfaces 2019, 11, 1321−1334

Table 1. Characterization Data of Representative Particles Used in This Study[a]

	PS1	PS2	SiO_2@PS1	SiO_2@PS2	GN-PS2	GN-CS
size (ecd)/nm	1254.2[b]	1282.6	1313.0[b]	1371.0	1314.5[c]	1368.5[c]
c_v	2.2[b]	3.3	2.5[b]	1.2	0.8[c]	1.9[c]
surface area/μm^2	4.95[d]	5.17[d]	9.53[e]	9.95	5.43[d]	10.43[e]
SiO_2 content (%)			n.d.[f]	19.8	n.d.[f]	n.d.[f]

[a]Diameter as equivalent circular diameter, ecd; coefficient of variation, c_v. GN = particle cores doped with green dye **1** (G) at concentrations N = 1−5 as specified in the respective section below; CS = core/shell. [b]Data taken from ref 40. [c]ecd and c_v were determined from ten line-scan measurements of particles from SEM images using ImageJ software. [d]Surface area of plain beads was calculated assuming an ideal sphere model. [e]Surface area was calculated using a factor of 1.92 (obtained from PS2 and SiO_2@PS2 data) and multiplying with surface area of plain beads. [f]Not determined due to low amount of encoded material.

ethanol was employed as solvent for the larger-scale batch to match the size of the particles of the two batches. This strategy was based on earlier findings of Paine's group, who observed that between methanol and butanol, an increase in the alcohol's chain length leads to larger particle sizes for such PS/PVP systems.[45] The respective PS particles in ref 39 and ref 40 had sizes of 0.94 and 1.25 μm. Accordingly, both syntheses led to particles of ∼1.3 μm diameter here (Table 1), termed PS2 (scaled-up batch in isopropanol) and PS1 (low-volume batch in ethanol). Both batches were obtained in good yields of 1.56 g (90.8%) for PS1 and 4.72 g (52.0%) for PS2. Whereas PS1 served as starting material for the surface modification experiments, PS2 was used for the encoding and immunoassay studies where higher amounts of material were necessary. Detailed information on the chemicals and protocols used are given in the Supporting Information, Section I.

Dye-Encoding of the PS Core. PS2 particles were encoded with hydrophobic BODIPY (boron−dipyrromethene) dyes (Chart 1)

Chart 1. Molecular Structures of Dyes 1 and 2

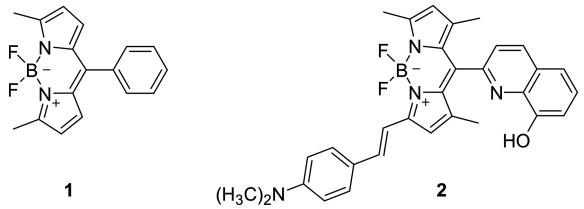

through an optimized two-step swelling technique in water/THF (tetrahydrofuran) mixtures. The two BODIPY dyes **1** and **2** were prepared according to published protocols.[46,47] First, 650 μL of particle stock dispersion (5% w/v) were mixed with 65 μL of pure THF for preswelling. After 1 h incubation at room temperature and gentle mixing using a rotator (40 rpm), 65 μL of the dye solution of the respective initial concentrations in THF were added and the combined solutions were further mixed for 2 h under identical conditions. Afterward, the beads were centrifuged and washed twice with water and once with ethanol (96%) in dispersion/centrifugation cycles. Finally, the beads were dried in a vacuum oven for 4 h and then stored in the dark at T < 10 °C. To create the 5-plex array, five different initial dye concentrations with 4, 2, 1, 0.5, and 0.25 × 10^{-4} M were used in accordance with the optimized working conditions. Details on the optimization of the doping procedure are given in the Supporting Information, Section II and Table S2.

SiO_2 Coating of Polymeric Core. The procedure for SiO_2 coating was adopted from ref 40. Dye-doped particles were coated in an Eppendorf tube, scaling down the volume of PS core dispersion to 1 mL (10 mg particles). Note that avoiding a magnetic stirrer and using vertical or overhead shaking is crucial to prevent destruction of the particles. Detailed information on the chemicals and protocols used are given in the Supporting Information, Section I.

Silica Shell Functionalization. Functionalization of the core/shell (CS) particles was performed after activation of the SiO_2 shell. Activation was done by ultrasonication of the particles for 5 min in a 1% w/v concentration using a 9:1 volume ratio of methanol and concentrated hydrochloric acid (HCl) as the dispersion medium. After washing the particles two times with ethanol in dispersion/centrifugation cycles, the beads were redispersed in the functionalization medium (either ethanol or water) to a stock concentration of 1% w/v for dye-encoded beads. Subsequently, the silane was added to the activated bead dispersion as a 1/10 diluted solution of APTES in ethanol (20 μL per 10 mg particles) to prepare unary surfaces. For binary surfaces, a 1/10 diluted solution of APTES in ethanol and a 1/5 diluted solution of PEGS in ethanol were subsequently added to the activated bead dispersion (20 μL per 10 mg particles each). Since the molecular weight of PEGS with ∼459 to ∼591 g mol^{-1} is almost twice as high as the MW of APTES with ∼221 g mol^{-1}, the mixture of the differently diluted silane solutions is quasi equimolar. The mixture was left to react at room temperature in a rotator (40 rpm) or at 40 °C in a thermomixer at 500 rpm. After 20 h reaction time, the particles were centrifuged and washed three times with ethanol and then left to dry in a vacuum oven for 3 h.

Caffeine Hapten (CAFH) Coupling. Particle dispersions (0.1% w/v) of CS beads were first prepared in 1.5 mL of absolute ethanol. Then, 50 μL of a 93 mM solution of *N*-hydroxysuccinimide (NHS)-activated ester of the caffeine hapten (CAFH, 7-(5-carboxypentyl)-1,3-dimethylxanthine) in dimethylformamide (DMF) were added and the mixture was left to react for 20 h in a thermomixer at room temperature at 500 rpm. The NHS activation of CAFH was done as reported by Carvalho et al.[48] After the reaction, the particles were centrifuged and washed three times with absolute ethanol in centrifugation/redispersion cycles. Finally, the particles were redispersed in 150 μL of $ethanol_{70\%}$ (∼1% w/v) and stored until further use as an array element in the bead-based immunoassay.

General Immunoassay Procedures. Immunoassays were performed in nonbinding, black microtiter plates (Greiner Bio-One). For dilution of the beads and biochemical reagents, TRIS buffered saline (10 mM tris(hydroxymethyl)aminomethane, 150 mM NaCl, pH = 8.5) was used. The incubation time for each step was set to 5 min, if not stated otherwise, and the plate was shaken at 750 rpm on an orbital shaker during incubation. Signal read-out was performed by flow cytometry, equipped with an autosampler for microtiter plates. A volume of 7 μL of each well was analyzed, using a flow rate of 14 μL min^{-1}. Beverage samples were degassed by ultrasonication and diluted 1:20 000 in ultrapure water (Milli-Q) prior to measurement. Details on the biochemical reagents used are given in Table S1.

Studies on Nonspecific Binding. In total, 100 μL of the primary antibodies (pAB) were incubated with 20 μL of a 0.00625% (w/v) suspension of CS particles for 5 min. For the indirect detection, 100 μL of AlexaFluor488-labeled secondary antibody (sAB) was additionally added and incubated for 25 min. A pair of an anti-CAF-AB (monoclonal mouse immunoglobulin G2b or IgG2B, clone 1.BB.877, Lot L2051502 M, US Biological, c = 0.14 μg mL^{-1}) and a goat anti-mouse IgG (H+L)-AlexaFluor488-sAB (polyclonal, Thermo Fisher Scientific, Lot 1745855, 2.0 μg mL^{-1}) served as a positive control for indirect detection. For direct detection, the anti-CAF-AB was fluorescently labeled using fluorescein isothiocyanate (FITC). A detailed labeling and purification procedure can be found in the Supporting Information. The obtained anti-CAF-FITC-AB was used in a concentration of 1.0 μg mL^{-1} and incubated with the beads for 30 min. In contrast, a FITC-labeled anti-bovine serum albumin-AB

DOI: 10.1021/acsami.8b10306
ACS Appl. Mater. Interfaces 2019, 11, 1321−1334

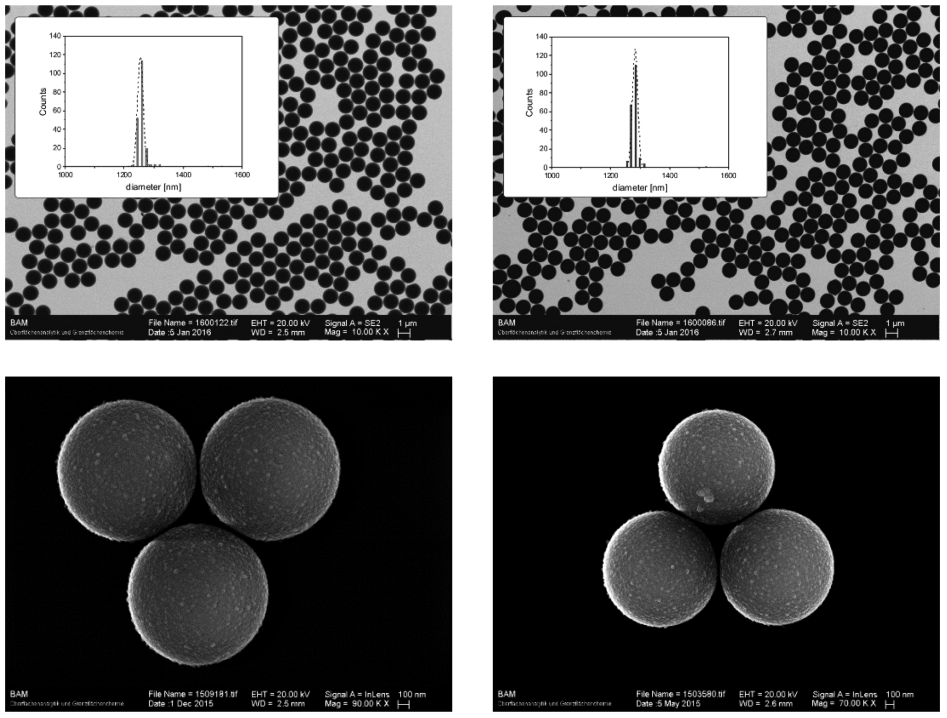

Figure 1. TSEM images of PS1 (top row, left) and PS2 (top row, right) in the same field of view (FOV); scale bars in lower right corners correspond to 1 μm. Insets: corresponding size distribution plots. Bottom row shows SEM images of three representative CS particles (SiO_2@PS1, left, and SiO_2@PS2, right) in different FOV; scale bars in lower right corners correspond to 100 nm.

(anti-BSA-AB, polyclonal, sheep, Thermo Fisher Scientific, 1.0 μg mL^{-1}) as well as a bovine-IgG (Sigma-Aldrich, 0.1 μg mL^{-1}) and an anti-bovine IgG(H+L)-AlexaFluor488-sAB (polyclonal, goat, Jackson ImmunoResearch, Lot 118210, 1.5 μg mL^{-1}) pair were used as negative control for CAFH-coupled beads.

Immunochemical Detection of PEG Surface Functionalization. For a first qualitative assessment of PEG moieties on the particles' surface, 100 μL of the primary anti-PEG antibodies (monoclonal rabbit IgG, clone PEG-B-47, abcam, 182 ng mL^{-1}) were incubated with 20 μL of a 0.0015% (w/v) suspension of CS particles for 5 min. After adding 100 μL of AlexaFluor488-labeled sAB (goat anti-rabbit IgG, polyclonal, Thermo Fisher Scientific, Lot 1745855, 2.0 μg mL^{-1}) and incubation for 25 min, the particles were analyzed by flow cytometry. Second, a seven-point titration curve of the anti-PEG-AB spanning from 90 to 0.001 ng mL^{-1}, using the same protocol, was recorded. Each point of the curve was measured in triplicate for unary (CS1) and binary (CS2) functionalized CS particles using EtOH and ultrapure water as a reaction medium.

Calibration Curves and Sample Measurements. A volume of 50 μL of either CAF standards in Milli-Q water or sample were incubated with 50 μL of anti-CAF-AB for 5 min. Then, 20 μL of a 0.00625% (w/v) suspension of differently encoded CS particles were added, before 100 μL of secondary, dye-labeled antibodies were added at a concentration of 2 μg mL^{-1}, followed by a 25 min incubation period. Depending on the dye used for encoding, either goat anti-mouse IgG (H+L)-AlexaFluor488-AB (for coding with red dye **2**) or goat anti-mouse IgG (H+L)-AlexaFluor647-AB (polyclonal, Thermo Fisher Scientific, Lot 1705800) (for coding with green dye **1**) were employed. Samples were measured in quadruplicate.

Fluorescence Spectroscopy. Fluorescence emission and excitation spectra of dye-encoded particles were recorded on a Fluoromax-4 spectrofluorometer (Horiba Scientific) with 0.05% (w/v) particle dispersions in water. Kinetic measurements to track code stability were conducted with a sample holder equipped with a magnetic stir bar (operated at 200 rpm) to avoid particle sedimentation during measurement. The signal intensity at λ_{em} = 525 nm for green- and λ_{em} = 650 nm for red-encoded beads was recorded at intervals of 1 s under irradiation at λ_{ex} = 489 nm (bandpass 3.5 nm) and λ_{ex} = 580 nm (bandpass 6.5 nm) for green- and red-encoded beads, respectively, over 30 min.

Flow Cytometry. A BD Accuri C6 was used with a typical optical setup and 488 nm as well as 635 nm lasers for excitation and fluorescence detection channels with 533/30 nm (FL1, green channel) and 675/25 nm (FL4, red channel) bandpass filters. Both spectral windows were used for decoding and analytical signal read-out with the respective encoding strategies and dye labels for detection. Signals were recorded as peak height, denoted as "-H", in the corresponding channels and are reported in mean channel intensity (MCI). Further details on signal treatment can be found in the Supporting Information, Section III and Figure S1.

RESULTS AND DISCUSSION

The core/shell format is ideally suited to build up composite systems that provide unique and novel features for multifunctional particles for bead-based analytical applications. The surface of a silica shell enables facile chemical tailoring with conventional silane chemistry.[49] The polymeric bead carrier defines the general properties (e.g., size, refractive index, and density) ideally required for handling and optical read-out. As the core material, two batches of similarly sized monodisperse PS particles obtained by dispersion polymerization with PVP40 as stabilizer were used. PS is the material of choice here because it allows facile control of bead size, possesses a high refractive index, and has a suitably low density for aqueous bead suspensions to remain stable. PVP acts as a binding agent to promote precipitation of silica seeds on the surface during the shell formation step.[50] One batch (PS1) was synthesized in a smaller scale, following ref 40. The surface modification studies were performed with this batch. The larger amounts of beads required for encoding and immunoassay studies were prepared according to ref 39 using isopropanol instead of ethanol as solvent (PS2). Both, PS1 and PS2 show diameters (ecd, equivalent circular diameter) of ~1.3 μm, possessing

DOI: 10.1021/acsami.8b10306
ACS Appl. Mater. Interfaces 2019, 11, 1321−1334

ideal sizes for bead-based applications (Figure 1, Table 1). The size was determined from scanning electron microscopy (SEM)-image analysis. To get statistically more reliable information on the particle size distribution of the samples, cytometric measurements were run and the forward scatter (FSC) plots analyzed. Figure S2 shows that both particle batches are highly monodisperse with c_v < 5%. The core/shell architecture was confirmed by SEM imaging after SiO_2 coating, revealing the typical raspberry-like structure already seen by us before (Figure 1, bottom row).[39,40] Transmission-mode SEM (TSEM) images revealed the typical, darker appearing shell domain for both batches and allowed one to derive the shell thicknesses (Figure S3, top row). For the large-scale batch, a shell thickness of roughly 40 nm is determined, while the smaller batch shows a shell thickness of 30 nm. The silica shell is composed of fused silica nanoparticles (SiO_2 NPs). Their diameters fit well to the measured shell thickness, indicating the formation of a closed monolayer-like assembly (Figure S3, bottom row). These shell thicknesses are confirmed indirectly by the differences of the diameters of the bare PS and the SiO_2@PS particles, divided by two (Table 1). An external surface area of for instance 9.95 $\mu m^2 \pm 0.98$ μm^2 per particle was calculated for SiO_2@PS2 by N_2 adsorption/desorption according to the t-plot method[51] of Lippens and de Boer using the Harkins and Jura correlation as described in ref 39. These values exceed the theoretical surface area of an (ideal) PS sphere of similar size (e.g., 5.17 μm^2 for PS2) by a factor of ~1.9. This increase in surface area reflects the formation of the raspberry-like shell structure. Assuming an equivalent surface increase for SiO_2@PS1 with similar shell structure, the surface area for SiO_2@PS1 was estimated as 9.53 μm^2. Further details on particle characterization are given in Section IV, Supporting Information.

Optical Encoding of the Polymeric Core. An essential requirement for beads to be applicable in multiplexed cytometric assays is their encoding. There are numerous possibilities to integrate unique identification features such as physical parameters (size, refractive index, shape) or optical codes.[52,53] The latter commonly rely on fluorescence properties immanent to the embedded luminophores such as nanoparticles (e.g., QDs, up-conversion NPs) or fluorescent dyes.[12,13,20] The optical code is used for identification of a specific type of bead equipped with a specific receptor unit or, as in this case, a specific analyte surrogate (hapten). The focus of our work lies on the possibility to simultaneously detect and quantify a comparably low number of analytes. This approach is most often sufficient in the monitoring of environmental compartments, agricultural processes, or the production of foodstuff. Because key problems are usually encountered when trying to use dyes for the generation of a larger library of codes, such as spectral cross-talk or concentration quenching which can be neglected here, we opted for simplicity, i.e., steric loading of organic dyes into the core by swelling.[43,54] Moreover, since bright and photostable BODIPY dyes are excellent candidates for such purposes[43,55] and our group has long-standing experience with BODIPY dyes,[46,56,57] we relied on two suitable dyes **1** and **2**. **1** emits green fluorescence and **2** emits red fluorescence that perfectly match with the optical layout of the conventional benchtop cytometer used here. Figure 2 depicts exemplary fluorescence excitation and emission spectra of encoded polymer beads PS2 (initial dye concentration of 2 × 10^{-4} M).

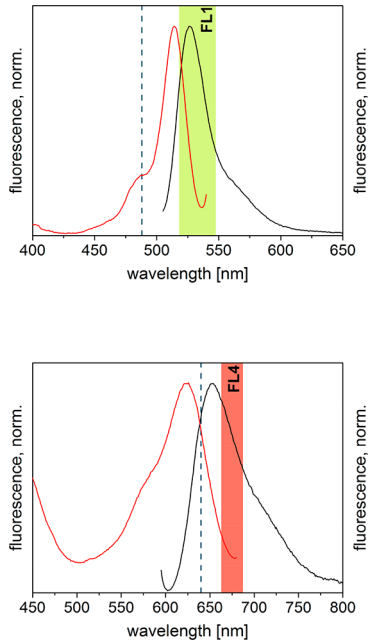

Figure 2. Emission (black, λ_{ex} = 489 and 580 nm) and excitation (red, λ_{obs} = 550 and 700 nm) spectra for green (top) and red (bottom) encoded polymer particles containing dyes **1** (top) and **2** (bottom). The vertical dashed lines denote the two laser wavelengths available in the cytometer, and the green and red areas are the spectral windows of the bandpass filters in the fluorescence channels FL1 and FL4 used here.

The use of **2**, a dye with a strongly solvatochromic emission, additionally provided insight into the polarity of the polystyrene matrix.[46] The emission maximum of 653 nm resembles closely that of **2** in diethyl ether, reflecting well the hydrophobic environment inside the PS core particles.

Creating a 5-Plex Array. After adaption of the dye-encoding procedure for PVP-stabilized PS cores, see Section II, Supporting Information, different concentrations of initial dye solution using green dye **1** (green; prefix "G") and red dye **2** (red; prefix "R") were employed to create five different codes (codes G1−G5 and codes R1−R5, using 4, 2, 1, 0.5, and 0.25 × 10^{-4} M dye stock solutions, respectively). The spectral properties of the encoded particles were investigated by fluorometry. The emission maximum of the green particles remained constant over all five concentrations, indicating unperturbed encapsulation of **1** without aggregation or the occurrence of reabsorption effects (Figure 3). In the case of the red particles, only the batch doped with the highest concentration of **2** (code R1) showed a slightly red-shifted emission band, indicative of minor reabsorption effects due to the high loading of the dye in the polymer matrix. However, this effect is negligible for the aspired application, and the entire set of beads was used in the further steps.

As Figure 4 shows, coating the doped PS core particles with silica has no detrimental effect and the green-encoded 5-plex CS particle array can be detected using flow cytometry. All particle populations can be well resolved in the fluorescence histogram plots (FL1-H and FL4-H) as well as in the correlation plot between FL1-H and FSC-H. For the red-encoded CS particles, slightly skewed profiles were observed with <4% of the events having been counted in the neighboring gate to lower intensities (Figure 4c,d). Although population separation is slightly worse than for the green

DOI: 10.1021/acsami.8b10306
ACS Appl. Mater. Interfaces 2019, 11, 1321−1334

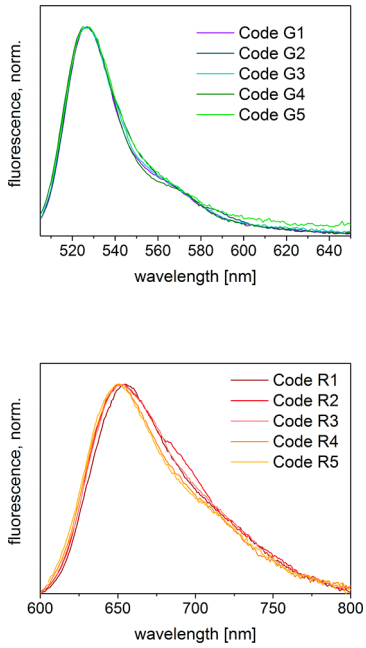

Figure 3. Normalized emission spectra of doped particle dispersions in water with different concentrations of dyes **1** (green-encoded, λ_{ex} = 489 nm, top) and **2** (red-encoded, λ_{ex} = 580 nm, bottom).

beads, >95% of correct binning, i.e., decoding allows us to use also the red beads for further studies. For both plex-sets, cross-talk between channels is negligible as evidenced by the only very low background fluorescence readings if, for instance, green-encoded beads were recorded in FL4 and red-encoded beads in FL1 (Figure S5). Hence, signal overlap between the fluorescence code and the analytical signal is virtually absent.

Excitation and emission spectra were recorded for encoded polymer and SiO_2-coated CS beads (codes G2, R2) to assess in more detail whether the coating influences the fluorescence properties of the embedded dyes (Figure 5). The overall spectral characteristics such as bandwidth and major band shape do not change, indicating that the dye remains intact during the silica coating process with its highly alkaline conditions.

The structural integrity of the CS particle 5-plex array was characterized by electron microscopy. Particles of each plex-set were mixed, including also nondoped CS beads, and SEM images were recorded. Figure 6 reveals that there is no significant difference between the green and the red 5-plex nor within one 5-plex set. This proves that a SiO_2 shell can successfully be grown onto pristine as well as dye-encoded particles without perturbing their features.

Dual Surface Functionalization of CS Beads and CAFH Coupling. To exploit the potential of rational surface design of CS beads, mixed silane surfaces using equimolar blends of APTES and PEG silane (PEGS) were prepared. PEG

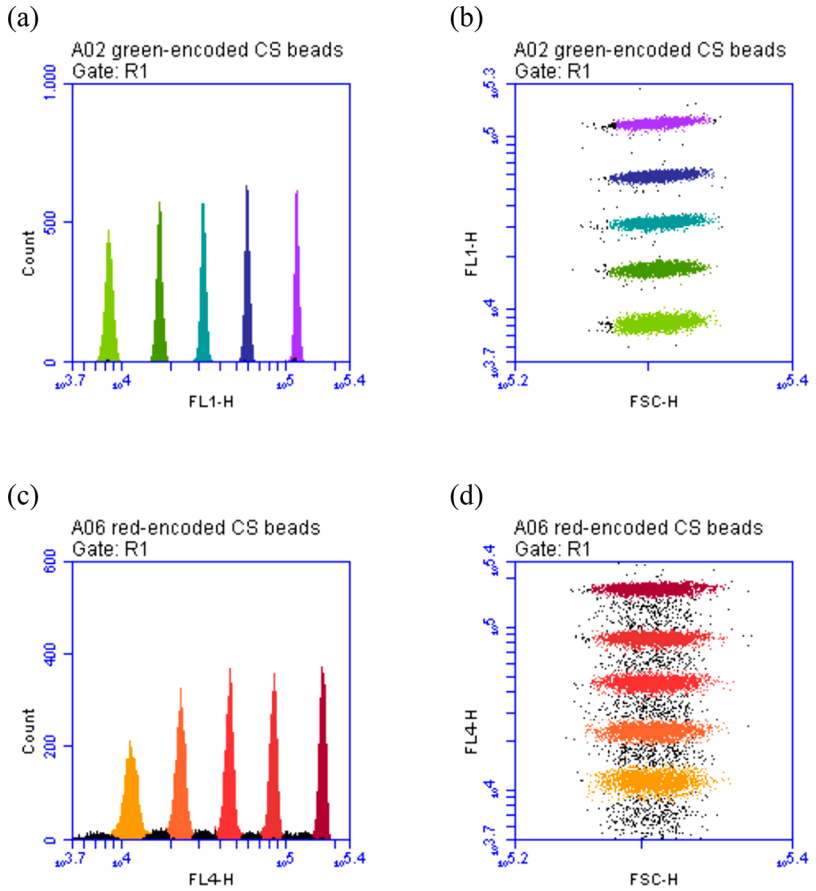

Figure 4. Gated and colored histograms and scatter plots for functionalized green-encoded (a,b) and red-encoded (c,d) CS beads in the respective decoding channel. Note that the functionalized encoded beads yield virtually identical patterns. (R1 = rectangular gate, see Supporting Information, Section III).

DOI: 10.1021/acsami.8b10306
ACS Appl. Mater. Interfaces 2019, 11, 1321−1334

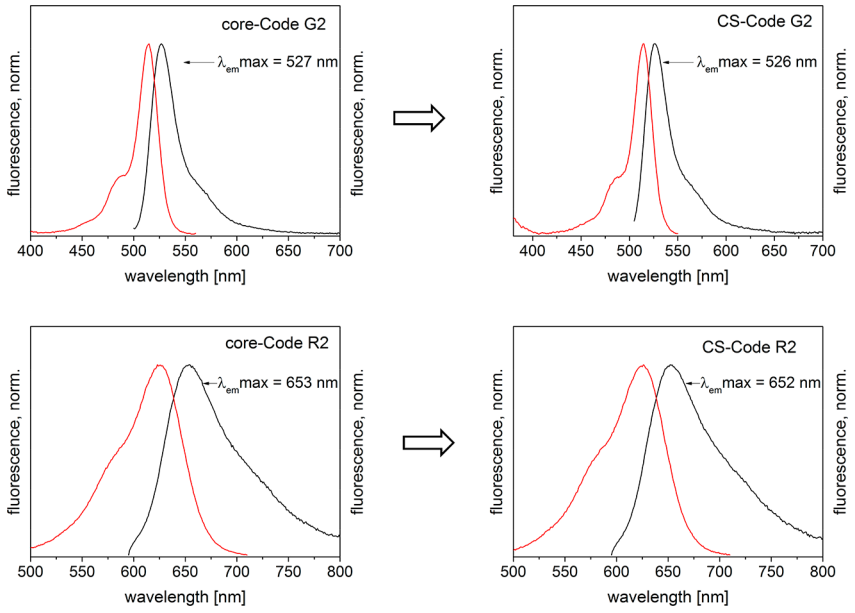

Figure 5. Fluorescence spectra for G2/R2-core (before coating) and G2/R2-CS (after coating) particles. Excitation spectra were recorded with λ_{obs} = 570 nm (top) and λ_{obs} = 730 nm (bottom) and emission spectra were recorded with λ_{ex} = 489 nm (top) and λ_{ex} = 580 nm (bottom) for green and red encoded particles, respectively.

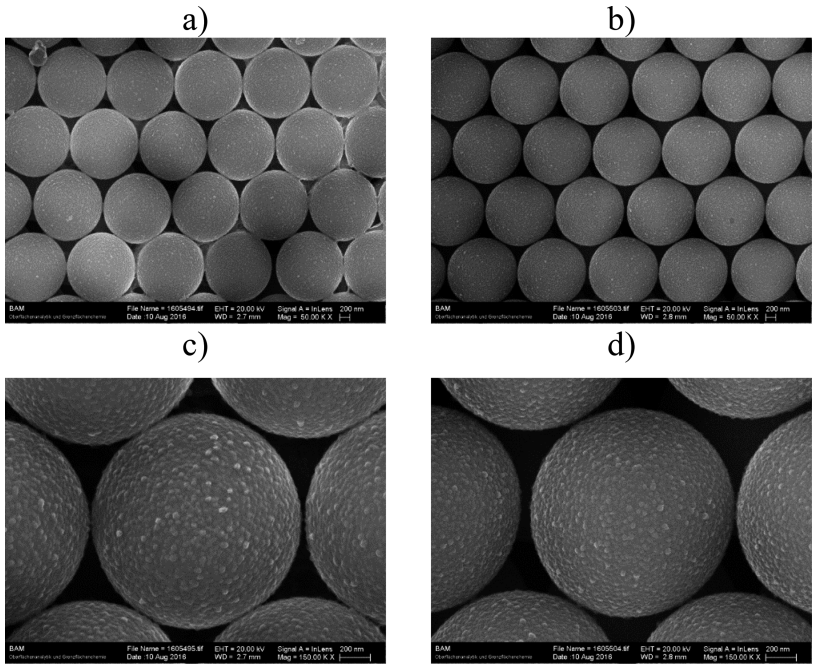

Figure 6. SEM images of the green- (a, c) and red- (b, d) encoded CS particles. For the green 5-plex, codes G1−G5 were mixed together in water, for the red 5-plex, codes R1−R5; scale bars correspond to 200 nm.

is widely known to suppress nonspecific binding of antibodies or other biomolecules because PEG moieties increase the hydrophilicity of flat or spherical surfaces.[58,59] In particular, APTES (unary surface as control, CS1) or an equimolar APTES/PEGS blend (binary surface, CS2) were simply added to preactivated CS beads in different solvents for functionalization without any additional catalyst. CAFH coupling was performed similarly for both particles CS1 and CS2 in a subsequent step, yielding CS1-CAFH and CS2-CAFH (Figure 7). SiO_2@PS1 beads were employed for the surface functionalization studies. Because the particles' polymer cores are not cross-linked, special attention must be paid to the silanization medium. Hydrophobic organic solvents will swell or even dissolve the polymeric core. Functionalization reactions are thus limited to either low MW alcohols or water as solvent. Consequently, two sets of particles with unary and binary surfaces were prepared in water at room temperature, ethanol at room temperature, and ethanol at 40 °C (EtOH40) to identify the best suitable functionalization conditions. Preactivation of the silica shell was carried out in a 9:1 methanol/HCl mixture, keeping the HCl content as low as possible to avoid etching of SiO_2.[60,61]

Mixed surfaces on silica shelled particles have so far only been prepared on silica-encapsulated inorganic nanoparticles

DOI: 10.1021/acsami.8b10306
ACS Appl. Mater. Interfaces 2019, 11, 1321−1334

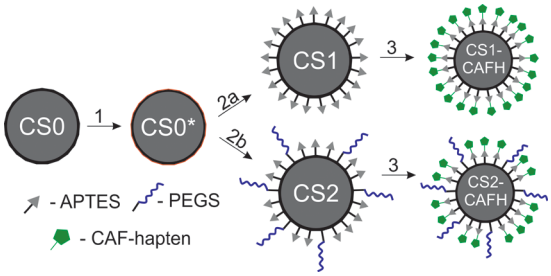

Figure 7. Schematic representation of particle activation (1) in MeOH/HCl, functionalization with unary APTES only (2a) as well as binary APTES/PEGS blend (2b) and coupling of CAFH (3).

(e.g., QDs and iron oxide NPs).[62,63] Our approach to mixed APTES/PEGS silane layers on dye-encoded SiO_2@PS particles for application in cytometric assays is thus original. In this study, we employed an equimolar ratio of APTES/PEGS, because preliminary tests with varying ratios and mixtures of silanes (including other organosilanes in ternary mixtures) showed no decisive influence on the antifouling properties. Future in-depth screening studies might lead to even better tailored beads, but as is evident from the results presented below, the equimolar mixture yields already highly potent objects.

Characterization of the Mixed Surfaces. All silane-functionalized particles possess positive zeta potentials, proving successful modification with APTES. In contrast, CS0 shows the characteristic negative zeta potential of a neat silica surface (Table S3, top row). The amount of amino groups on the CS particles was determined with a modified ninhydrin test.[64] Considering the calculated surface area of 9.53 μm^2 $particle^{-1}$, the amino group density was determined to ~11 APTES molecules per nm^2 for unary surfaces (Table S3, second row, entries for CS1). Such densities are typically found on spherical substrates due to the ability for denser packing or the formation of silane multilayers.[64] For binary surfaces prepared in ethanol, the total amino content per g of particles determined with the ninhydrin test is 22% lower compared to the unary surfaces (Table S3, third row, entries "EtOH40" and "EtOH" for CS2). For functionalization in water, however, the number of amino groups is even slightly higher for binary surfaces (Table S3, 2nd/3rd row, last column).

The quantitation of PEG on particle surfaces is challenging, especially when hybrid microparticles are under study.[65] This is why we aimed at a qualitative assessment of successful PEG grafting to the particles using an anti-PEG-AB in an indirect immunochemical test. Indeed, as we had hoped, the anti-PEG-AB bound to the rather short PEG chains immobilized on a hard sphere, rendering this method suitable for comparative assessment of grafting ratios. The assay results indicate that almost the same number of PEG groups are present on particles prepared in ethanol and water. This can be seen in Table S3, 4th row and in the very similar titration curves of the anti-PEG-AB with CS1 and CS2 particles prepared in either EtOH or water (Figure S6).

Subsequent CAFH grafting to both types of particles, i.e., those with single- and mixed-silane surfaces, yields comparably high conversion rates of amino groups, with coupling efficiencies between 78% and 90% (Table S3, bottom row). An indirect approach was chosen here, i.e., determination of the difference in amino group content prior to and after reaction of the beads with CAFH by ninhydrin tests as described above.

Inhibition of Nonspecific Binding Using Mixed Silane Layers. The effect of PEGS and/or APTES present on the surface of the CS1/CS2 particles and their influence on nonspecific binding of nontargeted antibodies was evaluated in a fit-for-purpose experiment. Therefore, a general model system was established: Positive and negative controls were carried out in a direct and an indirect fashion for CAFH-coupled particles and nonfunctionalized CS particles in cytometric immunoassays. The signals were detected after mixing the beads with a corresponding dye-labeled anti-CAF-AB (anti-caffeine antibody; direct) or anti-CAF-AB and dye-labeled sAB (secondary antibody; indirect). No washing steps were included because a mix-&-read assay was envisaged. Negative control responses were tested toward dye-labeled anti-BSA-AB (direct-negative) as well as with polyclonal bovine-IgG together with dye-labeled sAB (indirect-negative). In Figure 8, the four different immunochemical reactions are

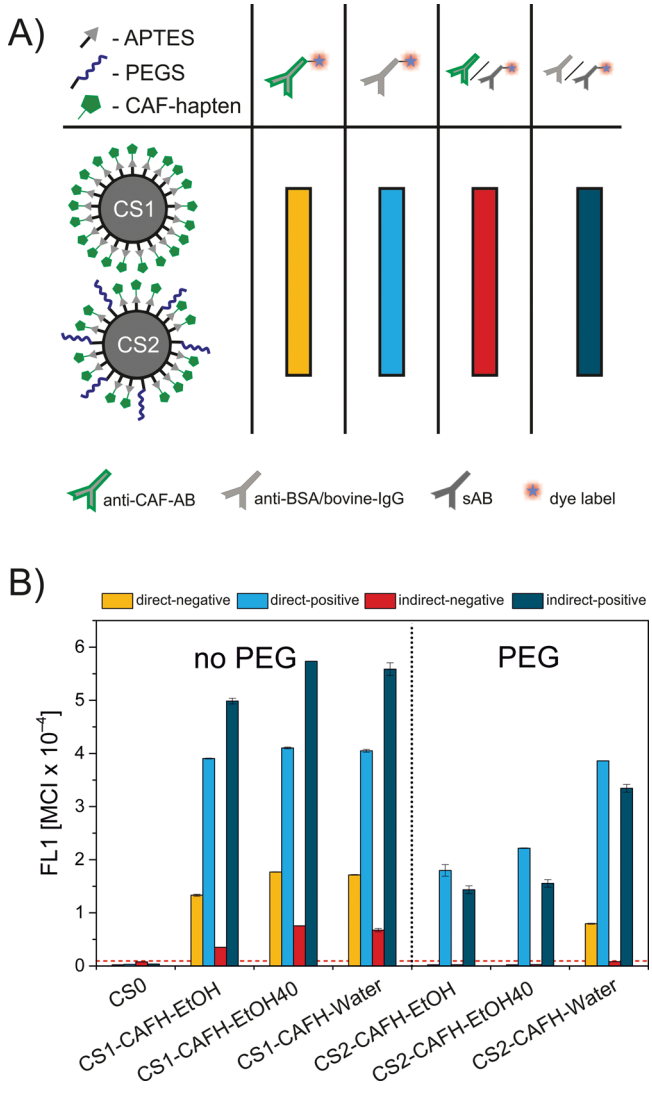

Figure 8. (A) Color code for the four different immunochemical reactions. (B) Cytometric assay results for CS0 as well as CS1 and CS2 after functionalization under different reaction conditions. The signal was recorded in FL1, and the standard deviations were obtained from triplicate measurements.

DOI: 10.1021/acsami.8b10306
ACS Appl. Mater. Interfaces 2019, 11, 1321−1334

assigned to a color code and the signal responses in the green channel FL1 are plotted in the lower part (for intensities, see Table S4). Note that the antibodies used here differ in clonality (mono- and polyclonal; anti-CAF-AB vs anti-BSA-AB) as well as in their origin (mouse and bovine; anti-CAF-AB vs bovine-IgG) to represent different classes of antibodies which are commonly used in immunoassays.

First, the control particles (CS0) with a neat silica surface show only weak signals in the direct and the indirect test, which proves the absence of nonspecific binding on native CS beads with an unmodified silica surface. The highest background signal of the CS0 series (indirect-negative test), plus 10 times the standard deviation of triplicate runs, was used as a threshold for false-positive signals in the other cases. Thus, signals from samples whose negative control exceeded an MCI of 962 (indicated as dashed red line) were classified as false-positive. To investigate the effect of silane functionalization on nonspecific binding, particles without CAFH modification were also tested. All responses are clearly below the false-positive benchmark, indicating that the zeta potential and therefore electrostatic interactions should have a minor influence on nonspecific binding (cf. Table S3, top row and Table S4, entries 1b−1e).

CS1-CAFH beads with unary surfaces in contrast, regardless of the functionalization conditions used, resulted in false-positive readings as well as high signal responses toward the respective pAB (primary antibody; anti-CAF-AB, anti-BSA-AB, or bovine IgG) for direct and indirect assays. The lowest false-positive signal (indirect negative, CS1-CAFH-EtOH) is still significantly higher than the background threshold. All other negative controls exceeded this value. Paired *t*-test analysis was used as a statistical hypothesis test and yielded a *t*-score $|t_{calc}| = 45.6$ and a probability $p = 1.4 \times 10^{-6}$ for 4 DF, degrees of freedom. The coupling of caffeine obviously leads to binding of the designated pAB, whether labeled or not. For nonlabeled pAB, tandem binding of sAB occurs readily as well. However, for both scenarios, nonspecific binding of nontargeted pABs is also considerably high (yellow and red bars in Figure 8, left panel "no PEG"). These data indicate that functionalization with CAFH is responsible for nonspecific binding, presumably due to the general reduction in polarity and hydrophilicity of the beads' surfaces when going from an APTES to a predominantly CAFH-coated surface.

The positive effect of PEGS can be deduced from binary CS2-CAFH beads functionalized in ethanol for which nonspecific binding, i.e., weak to none false-positive signals, was virtually absent for both, the direct and the indirect test (yellow and red bars in Figure 8, right panel "PEG"). The highest signal observed for negative controls (indirect negative, CS2-CAFH-EtOH40) was even significantly lower than the indirect negative test for neat silica surfaces, CS0 ($|t_{calc}| = 18.3$, $p = 5.2 \times 10^{-5}$, DF = 4). This indicates that the suppression of nonspecific interactions is distinctly higher for CS2-CAFH than for neat silica (CS0) and unary APTES-functionalized CS1-CAFH particles, the different CS1-CAFH showing signals above the preassigned threshold. Positive tests with 60- to 90-times higher signal intensities compared to the corresponding negative controls were found when the particles were functionalized in ethanol (Table S4, lines 5 and 6). When functionalization of CS2 beads was carried out in water (Table S4, line 7), however, the presence of PEG still suppresses nonspecific binding in the indirect assay, yet the signal gain is lower (only ∼40-fold) and a number of false-positive responses were registered in the direct assay, indicating worse selectivity against nontargeted polyclonal anti-BSA-AB. This finding is remarkable since the PEG content of these particles is comparable to that of the particles prepared in ethanol.

The adsorption behavior of APTES on silica surfaces might provide an explanation here. In aqueous solutions, as for CS1/CS2-Water, APTES tends to form monolayers due to electrostatic interaction between protonated amino groups and the negatively charged silanol-expressing surface.[66] Thus, shielding of the surface will perhaps prevent condensation of a less reactive second silane such as PEGS in the direct vicinity of the amino groups. Moreover, partial protonation of the amino groups in water would suppress their catalytic effect on the condensation of neighboring silanes. Instead, PEGS might preferentially condense at additional multilayer sites or in islands, leaving the total number of amino groups largely unchanged. As a result, the PEG chains might not be distributed homogeneously to evenly unfold their antifouling properties on the surface. On the other hand, for the CS2 particles functionalized in ethanol, the results show that nonspecific binding is suppressed. We assume that a more homogeneous mixture through APTES-catalyzed condensation of PEGS as proposed by Blitz et al. is responsible here.[67] Surface-bound APTES leads to the condensation of organosilanes in its proximity to form more homogeneous mixed silane layers.[67] In this case, PEG chains are evenly distributed within the silane layer, which is supported by the lower amount of APTES found on CS2 beads prepared in ethanol.

Encoded CS Particles with Dual Surface Functionalization. Ultimately, the best performing functionalization protocol, relying on ethanol (Figure 8), was adopted for the 5-plex bead set using SiO_2@PS2 to prepare multifunctional particles with a color code, functional group for coupling, and antifouling properties. It is worth mentioning that modifications of commercially available dye-encoded beads in ethanol would result in significant dye loss and destruction of the optical code. This would strongly limit the possibilities for chemical surface modification, because only reactions that can be conducted in neat aqueous media could be applied for the commercial beads. To assess the robustness of the title beads, dye leakage was tracked over the course of coating, functionalization, and hapten coupling along the optimized route with ethanol at room temperature (Figure S7a). A significant dye loss is only observed in the coating step, and the fluorescence code remains surprisingly stable during subsequent functionalization and hapten coupling steps in ethanol. The loss is therefore ascribed to hydrophobic TEOS acting as a swelling agent for the beads before its hydrolysis and the formation of the silica shell. This was confirmed by using a higher amount of TEOS (450 mM instead of 135 mM) during the coating of green-encoded beads, which led to a significant loss of dye/fluorescence intensity of ∼98%. It is also important to note that storage of beads in ethanol for >220 days led to only minor signal losses and still allowed for unequivocal resolution of the 5-plex in both cases, emphasizing the outstanding stability of the particles.

The photostability of codes G2 and R2 was also exemplarily investigated by tracking the fluorescence over time upon irradiation at 489 and 580 nm for green- and red-encoded beads (Figure S7b,c). A stabilizing effect of the silica shell was observed, which is ascribed to limited diffusion of oxygen into the beads, avoiding photo-oxidation.[68]

DOI: 10.1021/acsami.8b10306
ACS Appl. Mater. Interfaces 2019, 11, 1321−1334

Feasibility Study: Design of the Suspension Array Fluorescence Immunoassay. The working principle of the bead-based immunoassay devised by us in the present work is shown in Figure 9. It is a simple mix-&-read procedure based

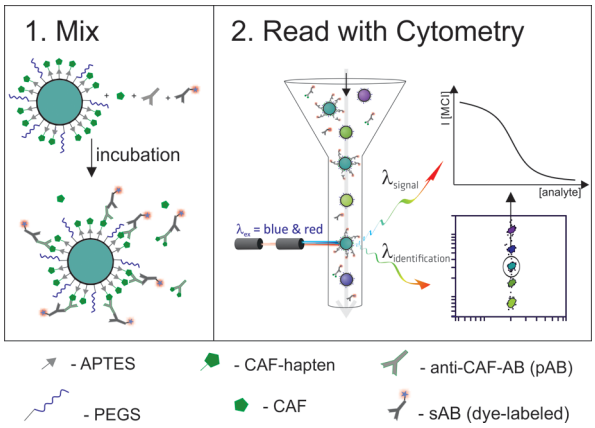

Figure 9. Principle of the CS particle-based assay using dye-encoded microbeads and indirect signal generation: (1) mixing and incubation and (2) reading and bead decoding by flow cytometry.

on our core/shell (CS) beads (using PS2 as starting material). The signal is generated on one particle (shown in bluish-green) in a mixture of differently encoded beads. Because each of the differently encoded beads can be associated with a specific immunoassay, the approach shall be perfectly suitable for multiplexing and the simultaneous detection of different small molecule analytes. This approach is a combination of the suspension array technology (SAT) and a fluorescence immunoassay (FIA). It is a simple, wash-free, and potentially multiplexable immunochemical test.

The signal generation relies on a competitive reaction between CAFH-bearing CS beads and the analyte present in the sample for the respective primary antibodies (pAB). Because the indirect assay format was applied, a dye-labeled secondary antibody (sAB) is added which binds to the pAB on the beads. All reagents are mixed in one compartment without additional washing steps and result in a competitive assay response. Using flow cytometry for signal read-out, bead-correlated fluorescence can be intrinsically discriminated from the background signal, i.e., from unbound labeled sAB. In this way, the analytical response can be detected without washing because nonspecific binding of proteins, such as primary or detection antibodies, on the designed bead surface carrying APTES/PEGS is efficiently suppressed.

Feasibility Study: Caffeine Detection in Beverages. Assay performance was tested with caffeine as a model analyte. First, a calibration curve was generated from the plex-set, mixing CAFH-conjugated CS2 particles (G3, R3) together with the four other nonconjugated CS particles. Eight fixed concentrations of CAF were then added together with pAB in triplicate. The signal response in detection channels FL1/FL4, stemming from the equivalent number of bound sABs, was recorded after incubation without washing. Figure 10 shows a representative data set generated by gating on the G3 bead population.

All signal responses remained below the 10σ threshold for nonlabeled beads, i.e., codes G1, G2, G4, and G5. Nonspecific binding is thus absent also within a mixture of all five encoded beads (Figure 10, middle). The residual black signal at higher

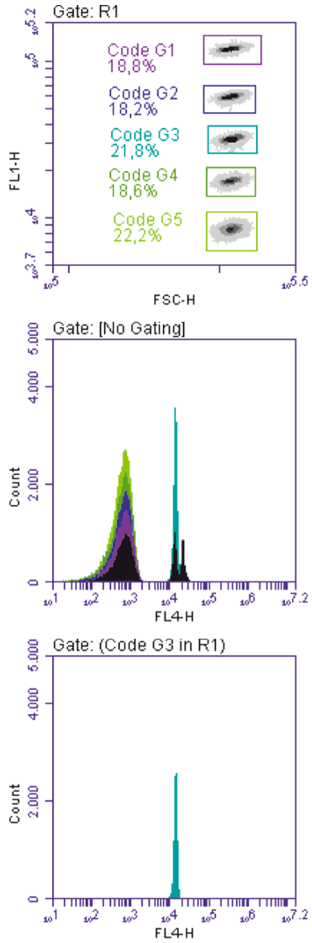

Figure 10. (Top) Color gates in the FL1-H vs FSC-H scatter plot (R1 gated). (Middle and bottom) Ungated and gated FL4-H detection channel readings for the lowest concentration of caffeine in the calibration measurement. The mean signal intensity from the gated plot (bottom) was used as the signal response of CS2 beads in the competitive assay. (R1 = rectangular gate, see Supporting Information, Section III.)

intensities in Figure 10, middle was tentatively attributed to aggregates which are not inside the rectangular gate R1 (see Supporting Information, Section III). These data will therefore not be considered in the subsequent analysis as can be seen in Figure 10, bottom. A logistic fit function (R^2 = 0.998) was used for analysis of the dose−response data (Figure 11, top). Working ranges (EC20−EC80) of 1.2−9.3 and 1.8−24 μg L^{-1} were determined for green- and red-encoded particles, respectively (Table S5). These are well suited for the detection of caffeine at low concentrations, for example, in beverages, after appropriate dilution.

As a proof of concept for a wash-free detection of small molecules in real samples, the content of CAF was measured in three different beverages (sample 1, Maya Mate; sample 2, Club Mate; and sample 3; Club Mate IceTea). The assay was performed without washing steps after a 1:20 000 dilution of the beverage in Milli-Q water, and the results are shown in Figure 11 (bottom). The data presented in Table S5 show that the CAF content could be determined with a mean recovery rate of 98 ± 31%, spanning from 68−146%, which is good for a simple, wash-free assay. Typically, SAT-based immunoassays yield recovery rates between 70−130%.[69−71] Most likely, fine-tuning of the incubation time, antibody concentrations, and

DOI: 10.1021/acsami.8b10306
ACS Appl. Mater. Interfaces 2019, 11, 1321−1334

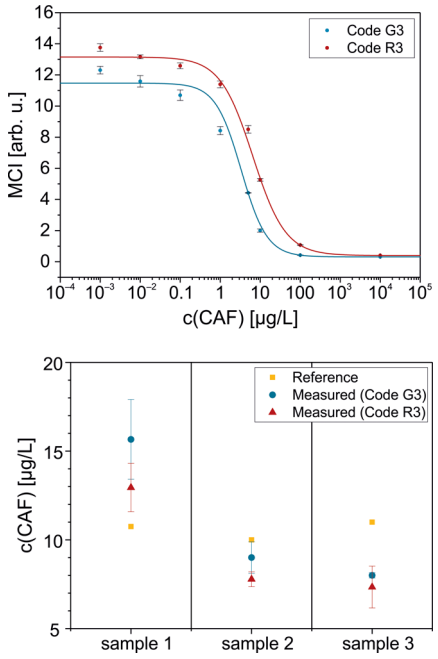

Figure 11. (Top) Calibration curve using a logistic fit function for analysis. (Bottom) CAF detection in 5-plex mixture with codes G3 and R3 in beverages (dilution factor, 1:20 000) with reference value shown in yellow.

buffer composition, hence classical immunoassay optimization loops, can further improve the assay performance of this format.

A factor which can influence the analytical result in wash-free assays is the incubation time associated with the detection delay when automated sample injection is utilized, for instance, from a 96-well plate as the multiple sample reservoir. In our model assay, a gradual increase of the signal response was indeed observed throughout the experiments, probably due to adsorption of sAB to the surface with progressing time or a nonequilibrium state. This effect can also be seen in the low-concentration response (Figure 11, top) where the signal does not reach saturation. Such kinetically induced shifts can be overcome using step-by-step sampling and measurement of each data point.

CONCLUSION

Rationally designed CS particles were successfully employed in the immunochemical detection of a low-molecular weight analyte molecule, using competitive binding of analyte and antigen-coupled microspheres to an anti-analyte-AB. The analytical signal was generated with a labeled secondary antibody and detected using a conventional two-laser benchtop cytometer.

The CS particles as solid supports have ideal material properties for cytometric detection and signal read-out. At the same time, the core acts as a matrix for encoding by doping with fluorescent dyes. Here, BODIPY dyes with different spectral properties were introduced to create five different optical codes each in the green and red detection channel. The polymeric core is thus fully compatible with classical encoding strategies while it still allows for an unperturbed growth of a silica shell on these dyed cores. Because of the versatility of BODIPY chemistry,[72] flexible color tuning can be realized in a straightforward manner.

The silica shell then adds unique benefit to the system because the surface can be precisely tuned using silane chemistry. In this study, simple silane blends with an equimolar ratio of APTES and PEGS were employed in an optimized functionalization procedure to prepare amino-functionalized mixed surfaces with antifouling properties. It was found that functionalization in ethanol gave superior performance over water. The procedure is a simple one-step co-condensation of an equimolar silane blend without requiring an additional catalyst. The presence of PEGS significantly reduced non-specific binding to the particles, facilitating quantification of the model analyte caffeine in a wash-free procedure.

Remarkably, only the stable encapsulation of dyes in CS particles which resist subsequent treatments and postmodification in ethanol solutions allowed to adapt the optimized protocol. Commercially available polymeric beads usually suffer from dye leaching when the particles are handled in ethanol. In future, other silanes could be tested in blends with APTES to tailor chemical or physical properties, such as adhesion, biocompatibility, charge, hydrophilicity/hydrophobicity of the particles, or introduce multiple functionalities on the surface.

This study shows the tremendous potential that resides with the solid support itself when using robust, easy-to-prepare hybrid particles consisting of polymeric cores with silica shells. Another major difference of this system to commercial platforms is the size. The CS particles with approximately 1.3 μm circular diameter are rather small in comparison to conventional beads with usually more than 3 μm. Nonetheless, their performance in a prototype assay was readily acceptable. Whereas for plain polystyrene beads of this size, particle handling would be cumbersome due to slow sedimentation speed, the title beads allowed for straightforward handling. Fast pelleting times (<2 min at 6 000 rpm) for washing and slow sedimentation for automated sampling (up to 2 h) are enabled due to the increased density of the hybrid material. Additionally, if using the same mass concentration, approximately 75-times more particles are present in the reaction chamber, which results in either less sample consumption to acquire the same number of beads or gives access to higher statistical numbers.

Current work in our laboratories is directed at the use of these multifunctional SiO_2@PS beads, carrying a color code in the core as well as bioconjugation and antifouling functionalities on the surface, in multiplexed small-molecule assays.

ASSOCIATED CONTENT

Supporting Information

The Supporting Information is available free of charge on the ACS Publications website at DOI: 10.1021/acsami.8b10306.

Details on materials, optimization of dye-encoding, flow cytometry, particle characterization as well as additional supporting data (PDF)

AUTHOR INFORMATION

Corresponding Author

*E-mail: knut.rurack@bam.de.

ORCID

Rudolf J. Schneider: 0000-0003-2228-1248

Knut Rurack: 0000-0002-5589-5548

DOI: 10.1021/acsami.8b10306
ACS Appl. Mater. Interfaces 2019, 11, 1321−1334

Author Contributions

The manuscript was written through contributions of all authors. All authors have given approval to the final version of the manuscript.

Funding

The MIS Program (BAM/BMWi, Grant No. Ideen_2012_14 to D.S. and Grant No. Ideen_2013_90 to P.C.) is acknowledged for funding.

Notes

The authors declare no competing financial interest.

■ ACKNOWLEDGMENTS

We thank Delia Gröninger and Jürgen Bartelmeß for synthetic support and Samual Burnage for fruitful discussions on bead synthesis and characterization.

■ REFERENCES

(1) Nolan, J. P.; Mandy, F. Multiplexed and Microparticle-Based Analyses: Quantitative Tools for the Large-Scale Analysis of Biological Systems. *Cytometry, Part A* **2006**, *69A* (5), 318−325.

(2) de Jager, W.; Rijkers, G. T. Solid-Phase and Bead-Based Cytokine Immunoassay: A Comparison. *Methods* **2006**, *38* (4), 294−303.

(3) Djoba Siawaya, J. F.; Roberts, T.; Babb, C.; Black, G.; Golakai, H. J.; Stanley, K.; Bapela, N. B.; Hoal, E.; Parida, S.; van Helden, P.; Walzl, G. An Evaluation of Commercial Fluorescent Bead-Based Luminex Cytokine Assays. *PLoS One* **2008**, *3* (7), No. e2535.

(4) Maltais, A.; Boye, J. I. Bead-Based Arrays: Multiplex Analyses. In *Green Technologies in Food Production and Processing*; Boye, J. I., Arcand, Y., Eds.; Springer, 2012.

(5) Nolan, J. P.; Sklar, L. A. Suspension Array Technology: Evolution of the Flat-Array Paradigm. *Trends Biotechnol.* **2002**, *20* (1), 9−12.

(6) Hsu, H.-Y.; Joos, T. O.; Koga, H. Multiplex Microsphere-Based Flow Cytometric Platforms for Protein Analysis and Their Application in Clinical Proteomics − from Assays to Results. *Electrophoresis* **2009**, *30* (23), 4008−4019.

(7) Yu, H. W.; Kim, I. S.; Niessner, R.; Knopp, D. Multiplex Competitive Microbead-Based Flow Cytometric Immunoassay Using Quantum Dot Fluorescent Labels. *Anal. Chim. Acta* **2012**, *750*, 191−198.

(8) Wang, Y.; Ning, B.; Peng, Y.; Bai, J.; Liu, M.; Fan, X.; Sun, Z.; Lv, Z.; Zhou, C.; Gao, Z. Application of Suspension Array for Simultaneous Detection of Four Different Mycotoxins in Corn and Peanut. *Biosens. Bioelectron.* **2013**, *41*, 391−396.

(9) Guo, Y.; Tian, J.; Liang, C.; Zhu, G.; Gui, W. Multiplex Bead-Array Competitive Immunoassay for Simultaneous Detection of Three Pesticides in Vegetables. *Microchim. Acta* **2013**, *180* (5), 387−395.

(10) Luminex. xMAP Technology, https://www.luminexcorp.com/eu/research-xmap-technology/ (accessed August 20, 2018).

(11) BD Biosciences. Bead-Based Immunoassays, https://www.bdbiosciences.com/in/research/cytometricbeadarray/ (accessed August 20, 2018).

(12) Wilson, R.; Cossins, A. R.; Spiller, D. G. Encoded Microcarriers For High-Throughput Multiplexed Detection. *Angew. Chem., Int. Ed.* **2006**, *45* (37), 6104−6117.

(13) Leng, Y.; Sun, K.; Chen, X.; Li, W. Suspension Arrays Based on Nanoparticle-Encoded Microspheres for High-Throughput Multiplexed Detection. *Chem. Soc. Rev.* **2015**, *44* (15), 5552−5595.

(14) Waterboer, T.; Sehr, P.; Pawlita, M. Suppression of Non-Specific Binding in Serological Luminex Assays. *J. Immunol. Methods* **2006**, *309* (1-2), 200−204.

(15) Zhu, Y.; Xu, H.; Chen, K.; Fu, J.; Gu, H. Encoding Through the Host-Guest Structure: Construction of Multiplexed Fluorescent Beads. *Chem. Commun.* **2014**, *50* (90), 14041−14044.

(16) Lu, S.; Zhang, D. S.; Wei, D.; Lin, Y.; Zhang, S.; He, H.; Wei, X.; Gu, H.; Xu, H. Three-Dimensional Barcodes with Ultrahigh Encoding Capacities: A Flexible, Accurate, and Reproducible Encoding Strategy for Suspension Arrays. *Chem. Mater.* **2017**, *29* (24), 10398−10408.

(17) Lu, Y.; Lu, J.; Zhao, J.; Cusido, J.; Raymo, F. M.; Yuan, J.; Yang, S.; Leif, R. C.; Huo, Y.; Piper, J. A.; Paul Robinson, J.; Goldys, E. M.; Jin, D. On-the-fly decoding luminescence lifetimes in the microsecond region for lanthanide-encoded suspension arrays. *Nat. Commun.* **2014**, *5*, 3741.

(18) Han, M.; Gao, X.; Su, J. Z.; Nie, S. Quantum-dot-tagged microbeads for multiplexed optical coding of biomolecules. *Nat. Biotechnol.* **2001**, *19* (7), 631−635.

(19) Bilan, R. S.; Krivenkov, V. A.; Berestovoy, M. A.; Efimov, A. E.; Agapov, I. I.; Samokhvalov, P. S.; Nabiev, I.; Sukhanova, A. Engineering of Optically Encoded Microbeads with FRET-Free Spatially Separated Quantum-Dot Layers for Multiplexed Assays. *ChemPhysChem* **2017**, *18* (8), 970−979.

(20) Birtwell, S.; Morgan, H. Microparticle Encoding Technologies for High-Throughput Multiplexed Suspension Assays. *Integr. Biol.* **2009**, *1* (5−6), 345−362.

(21) Falconnet, D.; She, J.; Tornay, R.; Leimgruber, E.; Bernasconi, D.; Lagopoulos, L.; Renaud, P.; Demierre, N.; van den Bogaard, P. Rapid, Sensitive and Real-Time Multiplexing Platform for the Analysis of Protein and Nucleic-Acid Biomarkers. *Anal. Chem.* **2015**, *87* (3), 1582−1589.

(22) Lee, H.; Kim, J.; Kim, H.; Kim, J.; Kwon, S. Colour-Barcoded Magnetic Microparticles for Multiplexed Bioassays. *Nat. Mater.* **2010**, *9* (9), 745−749.

(23) Lee, J.; Bisso, P. W.; Srinivas, R. L.; Kim, J. J.; Swiston, A. J.; Doyle, P. S. Universal Process-Inert Encoding Architecture for Polymer Microparticles. *Nat. Mater.* **2014**, *13* (5), 524−529.

(24) Juncker, D.; Bergeron, S.; Laforte, V.; Li, H. Cross-Reactivity in Antibody Microarrays and Multiplexed Sandwich Assays: Shedding Light on the Dark Side of Multiplexing. *Curr. Opin. Chem. Biol.* **2014**, *18*, 29−37.

(25) Dobosz, P.; Morais, S.; Bonet, E.; Puchades, R.; Maquieira, Á. Massive Immuno Multiresidue Screening of Water Pollutants. *Anal. Chem.* **2015**, *87* (19), 9817−9824.

(26) Pickering, J. W.; Larson, M. T.; Martins, T. B.; Copple, S. S.; Hill, H. R. Elimination of False-Positive Results in a Luminex Assay for Pneumococcal Antibodies. *Clin. Vaccine Immunol.* **2010**, *17* (1), 185−189.

(27) Lowe, S.; O'Brien-Simpson, N. M.; Connal, L. A. Antibiofouling Polymer Interfaces: Poly(ethylene glycol) and Other Promising Candidates. *Polym. Chem.* **2015**, *6* (2), 198−212.

(28) Kim, G.; Yoo, C. E.; Kim, M.; Kang, H. J.; Park, D.; Lee, M.; Huh, N. Noble Polymeric Surface Conjugated with Zwitterionic Moieties and Antibodies for the Isolation of Exosomes from Human Serum. *Bioconjugate Chem.* **2012**, *23* (10), 2114−2120.

(29) Pochechueva, T.; Chinarev, A.; Bovin, N.; Fedier, A.; Jacob, F.; Heinzelmann-Schwarz, V. PEGylation of Microbead Surfaces Reduces Unspecific Antibody Binding in Glycan-Based Suspension Array. *J. Immunol. Methods* **2014**, *412*, 42−52.

(30) Yuan, X.; Yoshimoto, K.; Nagasaki, Y. High-Performance Immunolatex Possessing a Mixed-PEG/Antibody Coimmobilized Surface: Highly Sensitive Ferritin Immunodiagnostics. *Anal. Chem.* **2009**, *81* (4), 1549−1556.

(31) Wattendorf, U.; Merkle, H. P. PEGylation as a Tool for the Biomedical Engineering of Surface Modified Microparticles. *J. Pharm. Sci.* **2008**, *97* (11), 4655−4669.

(32) Li, Y.; Wu, Y.; Luo, C.; Wang, B.; Wu, D. Rewritable Magnetic Fluorescence-Encoded Microspheres: Preparation, Characterization, and Recycling. *J. Mater. Chem. C* **2015**, *3* (31), 8262−8271.

(33) Wu, Y.; Li, Y.; Qin, L.; Yang, F.; Wu, D. Monodispersed or Narrow-Dispersed Melamine−Formaldehyde Resin Polymer Colloidal Spheres: Preparation, Size-Control, Modification, Bioconjugation and Particle Formation Mechanism. *J. Mater. Chem. B* **2013**, *1* (2), 204−212.

DOI: 10.1021/acsami.8b10306
ACS Appl. Mater. Interfaces 2019, 11, 1321−1334

(34) Wu, Y.; Li, Y.; Xu, J.; Wu, D. Incorporating Fluorescent Dyes into Monodisperse Melamine-Formaldehyde Resin Microspheres via an Organic Sol-Gel Process: a Pre-Polymer Doping Strategy. *J. Mater. Chem. B* **2014**, *2* (35), 5837−5846.
(35) Jun, B.-H.; Noh, M. S.; Kim, G.; Kang, H.; Kim, J.-H.; Chung, W.-J.; Kim, M.-S.; Kim, Y.-K.; Cho, M.-H.; Jeong, D. H.; Lee, Y.-S. Protein Separation and Identification Using Magnetic Beads Encoded with Surface-Enhanced Raman Spectroscopy. *Anal. Biochem.* **2009**, *391* (1), 24−30.
(36) Cao, Y.-C.; Huang, Z.-L.; Liu, T.-C.; Wang, H.-Q.; Zhu, X.-X.; Wang, Z.; Zhao, Y.-D.; Liu, M.-X.; Luo, Q.-M. Preparation of Silica Encapsulated Quantum Dot Encoded Beads for Multiplex Assay and Its Properties. *Anal. Biochem.* **2006**, *351* (2), 193−200.
(37) Caruso, F.; Möhwald, H. Preparation and Characterization of Ordered Nanoparticle and Polymer Composite Multilayers on Colloids. *Langmuir* **1999**, *15* (23), 8276−8281.
(38) Wilson, R.; Spiller, D. G.; Prior, I. A.; Veltkamp, K. J.; Hutchinson, A. A Simple Method for Preparing Spectrally Encoded Magnetic Beads for Multiplexed Detection. *ACS Nano* **2007**, *1* (5), 487−493.
(39) Sarma, D.; Gawlitza, K.; Rurack, K. Polystyrene Core−Silica Shell Particles with Defined Nanoarchitectures as a Versatile Platform for Suspension Array Technology. *Langmuir* **2016**, *32* (15), 3717−3727.
(40) Sarma, D.; Mielke, J.; Sahre, M.; Beck, U.; Hodoroaba, V.-D.; Rurack, K. TSEM-Based Contour Analysis as a Tool for the Quantification of the Profile Roughness of Silica Shells on Polystyrene Core Particles. *Appl. Surf. Sci.* **2017**, *426*, 446−455.
(41) Fischer, T.; Dietrich, P. M.; Streeck, C.; Ray, S.; Nutsch, A.; Shard, A.; Beckhoff, B.; Unger, W. E. S.; Rurack, K. Quantification of Variable Functional-Group Densities of Mixed-Silane Monolayers on Surfaces via a Dual-Mode Fluorescence and XPS Label. *Anal. Chem.* **2015**, *87* (5), 2685−2692.
(42) Fischer, T.; Dietrich, P. M.; Unger, W. E. S.; Rurack, K. Multimode Surface Functional Group Determination: Combining Steady-State and Time-Resolved Fluorescence with X-ray Photoelectron Spectroscopy and Absorption Measurements for Absolute Quantification. *Anal. Chem.* **2016**, *88* (2), 1210−1217.
(43) Descalzo, A. B.; Xu, H. J.; Xue, Z. L.; Hoffmann, K.; Shen, Z.; Weller, M. G.; You, X. Z.; Rurack, K. Phenanthrene-Fused Boron−Dipyrromethenes as Bright Long-Wavelength Fluorophores. *Org. Lett.* **2008**, *10* (8), 1581−1584.
(44) *Regulation (EU) No 1169/2011 of the European Parliament and of the Council on the Provision of Food Information to Consumers*, European Parliament and Council of the European Union: Brussels, Belgium, 2011.
(45) Paine, A. J.; Luymes, W.; McNulty, J. Dispersion Polymerization of Styrene in Polar-Solvents. 6. Influence of Reaction Parameters on Particle-Size and Molecular-Weight in Poly(N-vinylpyrrolidone)-Stabilized Reactions. *Macromolecules* **1990**, *23* (12), 3104−3109.
(46) Yu, Y.-H.; Descalzo, A. B.; Shen, Z.; Röhr, H.; Liu, Q.; Wang, Y.-W.; Spieles, M.; Li, Y.-Z.; Rurack, K.; You, X.-Z. Mono- and Di(dimethylamino)styryl-Substituted Borondipyrromethene and Borondiindomethene Dyes with Intense Near-Infrared Fluorescence. *Chem. - Asian J.* **2006**, *1* (1−2), 176−187.
(47) Qin, W.; Baruah, M.; Van der Auweraer, M.; De Schryver, F. C.; Boens, N. Photophysical Properties of Borondipyrromethene Analogues in Solution. *J. Phys. Chem. A* **2005**, *109* (33), 7371−7384.
(48) Carvalho, J. J.; Weller, M. G.; Panne, U.; Schneider, R. J. A Highly Sensitive Caffeine Immunoassay Based on a Monoclonal Antibody. *Anal. Bioanal. Chem.* **2010**, *396* (7), 2617−2628.
(49) Guerrero-Martinez, A.; Perez-Juste, J.; Liz-Marzan, L. M. Recent Progress on Silica Coating of Nanoparticles and Related Nanomaterials. *Adv. Mater.* **2010**, *22* (11), 1182−1195.
(50) Hong, J.; Han, H.; Hong, C. K.; Shim, S. E. A direct preparation of silica shell on polystyrene microspheres prepared by dispersion polymerization with polyvinylpyrrolidone. *J. Polym. Sci., Part A: Polym. Chem.* **2008**, *46* (8), 2884−2890.
(51) Lippens, B. C.; de Boer, J. H. Studies on Pore Systems in Catalysts. V. The t Method. *J. Catal.* **1965**, *4* (3), 319−323.
(52) Braeckmans, K.; De Smedt, S. C.; Leblans, M.; Pauwels, R.; Demeester, J. Encoding Microcarriers: Present and Future Technologies. *Nat. Rev. Drug Discovery* **2002**, *1* (6), 447−456.
(53) Kim, L. N.; Kim, M.; Jung, K.; Bae, H. J.; Jang, J.; Jung, Y.; Kim, J.; Kwon, S. Shape-Encoded Silica Microparticles for Multiplexed Bioassays. *Chem. Commun.* **2015**, *51* (60), 12130−12133.
(54) Behnke, T.; Würth, C.; Hoffmann, K.; Hübner, M.; Panne, U.; Resch-Genger, U. Encapsulation of Hydrophobic Dyes in Polystyrene Micro- and Nanoparticles via Swelling Procedures. *J. Fluoresc.* **2011**, *21* (3), 937−944.
(55) Wittmershaus, B. P.; Baseler, T. T.; Beaumont, G. T.; Zhang, Y.-Z. Excitation Energy Transfer from Polystyrene to Dye in 40-nm Diameter Microspheres. *J. Lumin.* **2002**, *96* (2), 107−118.
(56) Kollmannsberger, M.; Rurack, K.; Resch-Genger, U.; Daub, J. Ultrafast Charge Transfer in Amino-Substituted Boron Dipyrromethene Dyes and Its Inhibition by Cation Complexation: A New Design Concept for Highly Sensitive Fluorescent Probes. *J. Phys. Chem. A* **1998**, *102* (50), 10211−10220.
(57) Descalzo, A. B.; Xu, H.-J.; Shen, Z.; Rurack, K. Influence of the meso-Substituent on Strongly Red Emitting Phenanthrene-Fused Boron−Dipyrromethene (BODIPY) Fluorophores with a Propeller-Like Conformation. *J. Photochem. Photobiol., A* **2018**, *352*, 98−105.
(58) Anderson, A. S.; Dattelbaum, A. M.; Montaño, G. A.; Price, D. N.; Schmidt, J. G.; Martinez, J. S.; Grace, W. K.; Grace, K. M.; Swanson, B. I. Functional PEG-Modified Thin Films for Biological Detection. *Langmuir* **2008**, *24* (5), 2240−2247.
(59) Karakoti, A. S.; Das, S.; Thevuthasan, S.; Seal, S. PEGylated Inorganic Nanoparticles. *Angew. Chem., Int. Ed.* **2011**, *50* (9), 1980−1994.
(60) Cras, J. J.; Rowe-Taitt, C. A.; Nivens, D. A.; Ligler, F. S. Comparison of Chemical Cleaning Methods of Glass in Preparation for Silanization. *Biosens. Bioelectron.* **1999**, *14* (8−9), 683−688.
(61) Han, Y.; Mayer, D.; Offenhäusser, A.; Ingebrandt, S. Surface Activation of Thin Silicon Oxides by Wet Cleaning and Silanization. *Thin Solid Films* **2006**, *510* (1−2), 175−180.
(62) Goftman, V. V.; Aubert, T.; Ginste, D. V.; Van Deun, R.; Beloglazova, N. V.; Hens, Z.; De Saeger, S.; Goryacheva, I. Y. Synthesis, Modification, Bioconjugation of Silica Coated Fluorescent Quantum Dots and Their Application for Mycotoxin Detection. *Biosens. Bioelectron.* **2016**, *79*, 476−481.
(63) Hsu, J.-C.; Huang, C.-C.; Ou, K.-L.; Lu, N.; Mai, F.-D.; Chen, J.-K.; Chang, J.-Y. Silica Nanohybrids Integrated with CuInS2/ZnS Quantum Dots and Magnetite Nanocrystals: Multifunctional Agents for Dual-Modality Imaging and Drug Delivery. *J. Mater. Chem.* **2011**, *21* (48), 19257−19266.
(64) Soto-Cantu, E.; Cueto, R.; Koch, J.; Russo, P. S. Synthesis and Rapid Characterization of Amine-Functionalized Silica. *Langmuir* **2012**, *28* (13), 5562−5569.
(65) Rabanel, J.-M.; Hildgen, P.; Banquy, X. Assessment of PEG on Polymeric Particles Surface, a Key Step in Drug Carrier Translation. *J. Controlled Release* **2014**, *185*, 71−87.
(66) Kim, J.; Seidler, P.; Wan, L. S.; Fill, C. Formation, Structure, and Reactivity of Amino-Terminated Organic Films on Silicon Substrates. *J. Colloid Interface Sci.* **2009**, *329* (1), 114−119.
(67) Blitz, J. P.; Gun'ko, V. M.; Samala, R.; Lawrence, B. A. Mixed Bifunctional Surface-Modified Silicas Using Tethered Aminofunctional Silane Catalysts. *Colloids Surf., A* **2014**, *462*, 1−8.
(68) Kobayashi, Y.; Misawa, K.; Kobayashi, M.; Takeda, M.; Konno, M.; Satake, M.; Kawazoe, Y.; Ohuchi, N.; Kasuya, A. Silica-Coating of Fluorescent Polystyrene Microspheres by a Seeded Polymerization Technique and Their Photo-Bleaching Property. *Colloids Surf., A* **2004**, *242* (1−3), 47−52.
(69) Tsoi, T.-H.; Wong, W.-T. A Simple, Highly Sensitive, High Throughput and Organic Solvent-Free Screening Method for Melamine by Microsphere-Based Flow Cytometry Immunoassay. *Anal. Methods* **2015**, *7* (14), 5989−5995.

DOI: 10.1021/acsami.8b10306
ACS Appl. Mater. Interfaces 2019, 11, 1321−1334

(70) Jiang, X.; Zhu, Z.; Sun, Z.; Wang, L.; Zhou, L.; Miao, H.; Zhang, Z.; Shi, F.; Zhu, C. The Development of an Indirect Competitive Immunomagnetic-Proximity Ligation Assay for Small-Molecule Detection. *Analyst* **2013**, *138* (2), 438−442.
(71) Fraga, M.; Vilariño, N.; Louzao, M. C.; Rodríguez, P.; Campbell, K.; Elliott, C. T.; Botana, L. M. Multidetection of Paralytic, Diarrheic, and Amnesic Shellfish Toxins by an Inhibition Immunoassay Using a Microsphere-Flow Cytometry System. *Anal. Chem.* **2013**, *85* (16), 7794−7802.
(72) Loudet, A.; Burgess, K. BODIPY Dyes and Their Derivatives: Syntheses and Spectroscopic Properties. *Chem. Rev.* **2007**, *107* (11), 4891−4932.

DOI: 10.1021/acsami.8b10306
ACS Appl. Mater. Interfaces 2019, 11, 1321−1334